

Geometric speed limit for acceleration by natural selection in evolutionary processes

Masahiro Hoshino ^{1,*}, Ryuna Nagayama ^{1,2,†}, Kohei Yoshimura ^{1,2}, Jumpei F. Yamagishi ^{2,3} and Sosuke Ito ^{1,2}

¹Department of Physics, The University of Tokyo, 7-3-1 Hongo, Bunkyo-ku, Tokyo 113-0033, Japan

²Universal Biology Institute, The University of Tokyo, 7-3-1 Hongo, Bunkyo-ku, Tokyo 113-0033, Japan

³Graduate School of Arts and Sciences, The University of Tokyo, 3-8-1 Komaba, Meguro-ku, Tokyo 153-8902, Japan



(Received 13 July 2022; revised 13 January 2023; accepted 10 April 2023; published 26 May 2023)

We derived a new speed limit in population dynamics, which is a fundamental limit on the evolutionary rate. By splitting the contributions of selection and mutation to the evolutionary rate, we obtained the new bound on the speed of arbitrary observables, named the selection bound, that can be tighter than the conventional Cramér-Rao bound. Remarkably, the selection bound can be much tighter if the contribution of selection is more dominant than that of mutation. This tightness can be geometrically characterized by the correlation between the observable of interest and the growth rate. We also numerically illustrate the effectiveness of the selection bound in the transient dynamics of evolutionary processes and discuss how to test our speed limit experimentally.

DOI: [10.1103/PhysRevResearch.5.023127](https://doi.org/10.1103/PhysRevResearch.5.023127)

I. INTRODUCTION

Biological populations fluctuate through natural selection and mutation due to various environmental influences. While mutation increases their diversity, natural selection increases the fraction of highly adaptive traits in the population. This competition between selection and mutation leads to evolution [1–3]. Recent improvements in experimental methods have enabled researchers to quantitatively observe the evolutionary dynamics of actual biological communities [4–14]. For example, Ref. [9] visualized how selection and mutation together influence the adaptation dynamics of a bacterial population's growth.

Though these recent experiments allow us to measure the evolutionary rate quantitatively, the classical theories for evolution were not sufficiently quantitative. For example, the principal ideas of evolution, such as natural selection in Darwinian evolution [15], have not been clearly expressed quantitatively. A famous theorem on the evolutionary rate known as Fisher's fundamental theorem of natural selection [16–19], which claims a relation between the increment of the mean fitness and the fitness variance, has also been misunderstood by many researchers because it is given in a quantitatively vague expression [20]. One exception is the Price equation [20–26], which provides a clear-cut relation between the observables associated with traits and their fitness. Because the Price equation is a purely mathematical relation based on identity, we need to consider specific population

dynamics [27–30] to identify its physical implication for the evolutionary rate.

Recently, quantitative theoretical approaches have been developed by analogy with another developing field of stochastic thermodynamics [31,32]. In population dynamics models, such as the Lotka-Volterra model [33] and the lineage trees [34–37], several quantitative inequalities or trade-off relations for the evolutionary processes have been investigated [38–48] by analogy with thermodynamic laws such as the second law of thermodynamics [49,50] and thermodynamic uncertainty relations [51]. As a notable result, the evolutionary rate has been discussed quantitatively in Ref. [52] by applying the information-geometric speed limits [53,54]. The speed limits have been discussed as a classical counterpart of the quantum speed limits [55–61] in the context of a connection between information geometry [62] and stochastic thermodynamics. As a constraint on the speed of dynamics, the speed limits offer a basis to discuss the evolutionary rate quantitatively. These speed limits have also been generalized to the speed of observable [63–67] based on the Cramér-Rao bound [62,68], well known in information geometry. This information-geometric approach would be promising as a quantitative theory for the evolutionary rate because of a deep connection between the Cramér-Rao bound and the Price equation [25,26] and because this approach may be compatible with the existing information-theoretic and stochastic methods for evolutionary dynamics [69–78]. Indeed, several applications and generalizations of the speed limits have been recently studied to understand the speed in population dynamics quantitatively [79,80].

However, those previous studies [52,79,80] did not focus on the competing situations of natural selection and mutation, even though selection and mutation together shape evolution. Here we pose the following unresolved issue: *How and when does the evolutionary rate change in the competing situations of natural selection and mutation?* This question would be crucial for a quantitative understanding of evolutionary

*hoshino-masahiro921@g.ecc.u-tokyo.ac.jp

†ryuna.nagayama@ubi.s.u-tokyo.ac.jp

Published by the American Physical Society under the terms of the [Creative Commons Attribution 4.0 International](https://creativecommons.org/licenses/by/4.0/) license. Further distribution of this work must maintain attribution to the author(s) and the published article's title, journal citation, and DOI.

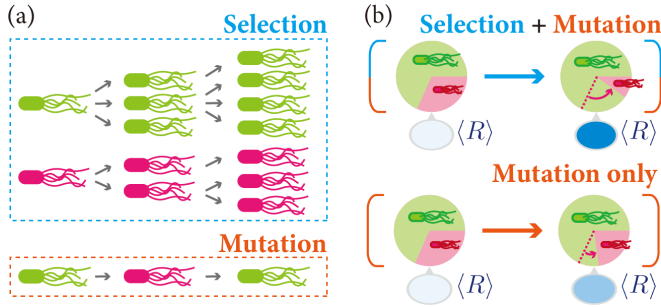


FIG. 1. (a) Schematic illustration of the model. Population size changes due to selection on growth and mutation. (b) Schematic illustration of the selection bound. Compared to the case where the population changes only due to mutation, the change of $\langle R \rangle$ can be accelerated when both selection and mutation affect the population dynamics.

processes where the competition between selection and mutation can enhance the evolutionary rate, as observed in Ref. [9].

To resolve such an issue, we theoretically evaluated the evolutionary rate by decomposing it into the contributions of natural selection and mutation in population dynamics, thereby deriving a new speed limit. This speed limit is tighter than the conventional Cramér-Rao bound when natural selection is dominant compared to mutation (e.g., in transient dynamics of evolution), as analytically proven and numerically illustrated. It describes how natural selection accelerates evolution.

II. POPULATION DYNAMICS

A. Setup

To discuss speed limits for observables in population dynamics, we consider a model consisting of selection and mutation between multiple traits [29] [see also Fig. 1(a)]. Suppose a population consists of subpopulations with n different traits, and $N_i(t)$ and λ_i denote the number and growth rate of individuals in the subpopulation with the i th trait at time t , respectively. The traits may be phenotypic, genotypic, or epigenetic properties. We denote the vector of growth rates simply as $\lambda = (\lambda_i)$. Mutation is assumed to be a Markovian process with transition rate matrix $\mathbf{W} = (W_{ij})$, where the (i, j) -element W_{ij} indicates the transition rate from trait j to i if $i \neq j$, and the elements satisfy $\sum_{i=1}^n W_{ij} = 0$ and $W_{ij} \geq 0$ ($i \neq j$). We assume that λ and \mathbf{W} are time independent because we consider a stationary environment. Then $N_i(t)$ follows the following differential equation:

$$\frac{d}{dt}N_i(t) = \lambda_i N_i(t) + \sum_{j=1}^n W_{ij} N_j(t). \quad (1)$$

The first term on the right-hand side represents the change in the population due to selection and the second term represents the change in the population due to mutation. With $N_{\text{tot}}(t) := \sum_{i=1}^n N_i(t)$, the proportion $p_i(t) := N_i(t)/N_{\text{tot}}(t)$ of each subpopulation satisfies the definition of the probability distribution, i.e., the non-negativity $p_i(t) \geq 0$ and the normalization $\sum_{i=1}^n p_i(t) = 1$. From Eq. (1), this ‘‘probability

distribution’’ follows a nonlinear master equation,

$$\frac{d}{dt}p_i(t) = \Delta\lambda_i p_i(t) + \sum_{j=1}^n W_{ij} p_j(t), \quad (2)$$

where the ensemble average of an observable $A = \{A_i\}_{i=1}^n$ with respect to $p_i(t)$ is defined as $\langle A \rangle := \sum_{i=1}^n p_i(t) A_i$ and $\Delta A_i = A_i - \langle A \rangle$ denotes the deviation of A_i .

B. Speed limit and information geometry

We here briefly explain the conventional information-geometric speed limit for a time-independent observable $R = \{R_i\}_{i=1}^n$. The speed of observable R is defined as

$$v_R := \frac{1}{\sqrt{\text{Var}[R]}} \frac{d\langle R \rangle}{dt}, \quad (3)$$

where $\text{Var}[R] := \langle (\Delta R)^2 \rangle$ is the variance of R . In population dynamics, v_R quantifies the evolutionary rate with respect to observable R . For example, the evolutionary rate with respect to the growth rate, v_λ , is given by the time derivative of the averaged growth rate $d\langle \lambda \rangle / dt$ normalized by its standard deviation $\sqrt{\text{Var}[\lambda]}$. The speed limit for observable, known as the Cramér-Rao bound, is a universal constraint on this speed v_R for any observable R [63,64]:

$$-v_{\text{info}} \leq v_R \leq v_{\text{info}}, \quad (4)$$

which holds for arbitrary dynamics of a probability distribution [81]. Here v_{info} is defined as the square root of the Fisher information [63,82,83]:

$$v_{\text{info}} := \sqrt{\sum_{i=1}^n p_i \left(\frac{d \ln p_i}{dt} \right)^2}. \quad (5)$$

In information geometry, we can interpret it as the speed of a probability distribution moving on a manifold of distributions.

C. Fitness and Price equation

The square root of the Fisher information v_{info} not only indicates the speed of the probability distribution but also characterizes the population dynamics because it is identified with the variance of fitness [19,25]. We here introduce the fitness f_i of trait i as the effective growth rate of N_i :

$$f_i := \frac{d}{dt} \ln N_i(t). \quad (6)$$

The ensemble average of the fitness is equal to the effective growth rate of the total population: $\langle f \rangle = d \ln N_{\text{tot}} / dt$. Together with Eq. (5) and $\ln p_i(t) = \ln N_i(t) - \ln N_{\text{tot}}(t)$, these relations lead to the equality

$$v_{\text{info}} = \sqrt{\sum_{i=1}^n p_i (\Delta f_i)^2} = \sqrt{\text{Var}[f]}. \quad (7)$$

That is, v_{info} also quantifies the diversity of each trait’s fitness. Accordingly, Eq. (4) implies that the variance of fitness limits the speed of an arbitrary observable.

On the other hand, we can discuss the role of v_R in population dynamics based on the Price equation [20–26]. A special case of the Price equation for a time-independent observable

provides a connection with the time derivative of the stochastic entropy in the system, $\dot{\sigma}_i(t) := -d \ln p_i(t)/dt$, as

$$\frac{d\langle R \rangle}{dt} = \text{Cov}[R, -\dot{\sigma}], \quad (8)$$

where the covariance of two observables is defined as $\text{Cov}[A, B] := \langle \Delta A \Delta B \rangle$. This equation indicates that the evolutionary rate is governed by the stochastic entropy change rate in the system. We remark that $\dot{\sigma}$ is directly connected to the fitness as $-\dot{\sigma}_i = \Delta f_i$, so that its ensemble average and variance satisfy $\langle \dot{\sigma} \rangle = 0$ and $\sqrt{\text{Var}[\dot{\sigma}]} = \sqrt{\text{Var}[f]} = v_{\text{info}}$. From Eq. (8), v_R is rewritten as

$$v_R = \frac{\text{Cov}[R, -\dot{\sigma}]}{\sqrt{\text{Var}[R]}} = \frac{\text{Cov}[R, f]}{\sqrt{\text{Var}[R]}}, \quad (9)$$

which implies that the speed of an observable can be interpreted in terms of the covariance between the observable and the fitness. From Eqs. (7) and (9), the Cramér-Rao bound (4) can be derived by applying the Cauchy-Schwarz inequality $-\sqrt{\text{Var}[R]}\sqrt{\text{Var}[f]} \leq \text{Cov}[R, f] \leq \sqrt{\text{Var}[R]}\sqrt{\text{Var}[f]}$.

III. GEOMETRIC SPEED LIMIT FOR ACCELERATION BY SELECTION

A. Main result: Selection bound

We explain the main result which is a new speed limit based on the contribution of selection in evolutionary dynamics. The key idea for the main result is the decomposition of the stochastic entropy change rate in the system. In the population dynamics model (2), $\dot{\sigma}$ can be decomposed into two parts as

$$\dot{\sigma} = \dot{\sigma}^\lambda + \dot{\sigma}^W, \quad (10)$$

where $\dot{\sigma}_i^\lambda := -\Delta \lambda_i$ and $\dot{\sigma}_i^W := -\sum_{j=1}^n W_{ij} p_j / p_i$ are the stochastic entropy change rate in the system due to only selection and mutation, respectively. We remark that $\dot{\sigma}^W$ is rewritten as $\dot{\sigma}_i^W = -\Delta(f_i - \lambda_i)$. These quantities also satisfy $\langle \dot{\sigma}^\lambda \rangle = \langle \dot{\sigma}^W \rangle = 0$, as $\dot{\sigma}$ does. Considering this decomposition, we introduce the following quantities:

$$\begin{aligned} v_R^\lambda &:= \frac{\text{Cov}[R, -\dot{\sigma}^\lambda]}{\sqrt{\text{Var}[R]}}, & v_{\text{info}}^\lambda &:= \sqrt{\text{Var}[\dot{\sigma}^\lambda]}, \\ v_R^W &:= \frac{\text{Cov}[R, -\dot{\sigma}^W]}{\sqrt{\text{Var}[R]}}, & v_{\text{info}}^W &:= \sqrt{\text{Var}[\dot{\sigma}^W]}, \end{aligned} \quad (11)$$

where the upper two can be interpreted as v_R and v_{info} without the contribution of mutation, while the lower ones are interpreted as those without selection. In other words, the former are speeds stemming solely from selection, while the latter mutation only. These quantities are given by the variance and covariance of the measurable observables R , λ , and $f - \lambda$; $v_R^\lambda = \text{Cov}[R, \lambda] / \sqrt{\text{Var}[R]}$, $v_{\text{info}}^\lambda = \sqrt{\text{Var}[\lambda]}$, $v_R^W = \text{Cov}[R, f - \lambda] / \sqrt{\text{Var}[R]}$, and $v_{\text{info}}^W = \sqrt{\text{Var}[f - \lambda]}$. By decomposing v_R into the contributions of selection and mutation, we obtain a new speed limit:

$$v_R^\lambda - v_{\text{info}}^W \leq v_R \leq v_R^\lambda + v_{\text{info}}^W. \quad (12)$$

We call this new speed limit *the selection bound* because the speed of observable v_R is accelerated by the effect of

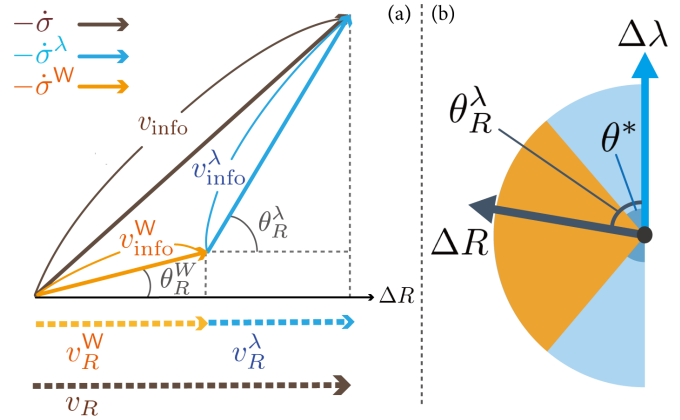


FIG. 2. (a) Relations between the quantities presented in this paper in the inner product space. $-\dot{\sigma}$ can be written by the sum of the contributions of selection and mutation, $-\dot{\sigma}^\lambda$ and $-\dot{\sigma}^W$. The norms of $-\dot{\sigma}$, $-\dot{\sigma}^\lambda$, $-\dot{\sigma}^W$ are v_{info} , v_{info}^λ , v_{info}^W , respectively. The speed v_R can be expressed by the projection of $-\dot{\sigma}$ in the direction of ΔR , while the projections of $-\dot{\sigma}^\lambda$ and $-\dot{\sigma}^W$ are v_R^λ and v_R^W , respectively. Thus, $v_R = v_R^\lambda + v_R^W$ holds. (b) The range of θ_R^λ that determines whether the selection bound or the Cramér-Rao bound evaluates v_R tightly or loosely. If $\theta^* \leq \theta_R^\lambda \leq \pi$, then the selection bound gives a tighter upper bound, and if $0 \leq \theta_R^\lambda \leq \pi - \theta^*$, then the selection bound gives a tighter lower bound. Therefore, both upper and lower bounds are tight when θ_R^λ is located in the orange area $[\theta^*, \pi - \theta^*]$.

selection v_R^λ , compared to the case where no selection occurs ($-v_{\text{info}}^W \leq v_R \leq v_{\text{info}}^W$ for $\lambda = 0$). Therefore, this bound quantifies the acceleration of the evolutionary rate by natural selection compared to mutational dynamics in the absence of the selection [see also Fig. 1(b)].

The equation (12) is derived essentially from the Cauchy-Schwarz inequality as well as the Cramér-Rao bound. To simplify its derivation, we define an inner product and the associated norm for observables as $\langle A, B \rangle := \sum_{i=1}^n p_i A_i B_i$ and $\|A\| := \sqrt{\langle A, A \rangle}$, respectively. We can rewrite v_R as

$$v_R = \frac{\langle \Delta R, \Delta \lambda + \Delta(f - \lambda) \rangle}{\|\Delta R\|} = v_R^\lambda + v_R^W. \quad (13)$$

Applying the Cauchy-Schwarz inequality $-\|\Delta R\| \|\Delta(f - \lambda)\| \leq \langle \Delta R, \Delta(f - \lambda) \rangle \leq \|\Delta R\| \|\Delta(f - \lambda)\|$ to Eq. (13), we can obtain the selection bound.

This inner product also provides a useful geometric interpretation to discuss the effectiveness of the selection bound [see also Fig. 2(a)]. In the geometric interpretation, $v_{\text{info}} = \|\dot{\sigma}\|$, $v_{\text{info}}^\lambda = \|\dot{\sigma}^\lambda\|$, and $v_{\text{info}}^W = \|\dot{\sigma}^W\|$ are the norms of $-\dot{\sigma}$, $-\dot{\sigma}^\lambda$, and $-\dot{\sigma}^W$, respectively, and thus the triangle inequality $|v_{\text{info}}^\lambda - v_{\text{info}}^W| \leq v_{\text{info}} \leq v_{\text{info}}^\lambda + v_{\text{info}}^W$ holds. In addition, $v_R = \langle \Delta R, -\dot{\sigma} \rangle / \|\Delta R\|$, $v_R^\lambda = \langle \Delta R, -\dot{\sigma}^\lambda \rangle / \|\Delta R\|$, and $v_R^W = \langle \Delta R, -\dot{\sigma}^W \rangle / \|\Delta R\|$ are the norms of the projections of $-\dot{\sigma}$, $-\dot{\sigma}^\lambda$, and $-\dot{\sigma}^W$ onto ΔR , respectively. Then, the angle between ΔR and $-\dot{\sigma}^\lambda = \Delta \lambda$ can be defined as

$$\theta_R^\lambda := \arccos \left(\frac{\langle \Delta R, \Delta \lambda \rangle}{\|\Delta R\| \|\Delta \lambda\|} \right) = \arccos \left(\frac{v_R^\lambda}{v_{\text{info}}^\lambda} \right), \quad (14)$$

or equivalently $v_R^\lambda = v_{\text{info}}^\lambda \cos \theta_R^\lambda$. It quantifies the strength of the correlation between R and λ [84]. If there is a positive correlation between an observable R and the growth rate λ

(i.e., $\cos \theta_R^\lambda \geq 0$), then v_R^λ is positive and both upper and lower bounds in the selection bound shift to the positive direction (i.e., $\pm v_{\text{info}}^W + v_R^\lambda$), compared to the case without selection (i.e., $\pm v_{\text{info}}^W$). Therefore, positive correlations between observables and the growth rate can lead to faster evolution. From a biological viewpoint, it indicates that if the value of the observable R tends to be larger in fast-growing traits, then its evolutionary rate can be accelerated, and vice versa. Noting the relation $v_R^\lambda = v_{\text{info}}^\lambda \cos \theta_R^\lambda$, not only stronger correlations between observables and growth rate (i.e., larger $\cos \theta_R^\lambda$) but also greater contributions of selection (i.e., larger v_{info}^λ , as discussed above) together allow a faster evolutionary rate.

Finally, let us compare our bound (12) with the conventional Cramér-Rao bound (4) to see how it quantifies the competition between selection and mutation. To this end, we define another angle θ^* as

$$\theta^* := \arccos \left(\frac{v_{\text{info}} - v_{\text{info}}^W}{v_{\text{info}}^\lambda} \right), \quad (15)$$

which is well defined because the argument of the arccosine is always in $[-1, 1]$ from the triangle inequality. Using θ_R^λ and θ^* , the following case separation gives the condition in which case the Cramér-Rao bound or the selection bound gives better evaluation (see Appendix A for the derivation):

$$\begin{aligned} 0 \leq \theta_R^\lambda \leq \theta^* &\Rightarrow v_R \leq v_{\text{info}} \leq v_R^\lambda + v_{\text{info}}^W \\ \theta^* \leq \theta_R^\lambda \leq \pi &\Rightarrow v_R \leq v_R^\lambda + v_{\text{info}}^W \leq v_{\text{info}} \\ 0 \leq \theta_R^\lambda \leq \pi - \theta^* &\Rightarrow -v_{\text{info}} \leq v_R^\lambda - v_{\text{info}}^W \leq v_R \\ \pi - \theta^* \leq \theta_R^\lambda \leq \pi &\Rightarrow v_R^\lambda - v_{\text{info}}^W \leq -v_{\text{info}} \leq v_R. \end{aligned} \quad (16)$$

This implies that if θ^* is smaller than $\pi/2$ and θ_R^λ is in the range $[\theta^*, \pi - \theta^*]$, then the selection bound will bound v_R more tightly than the Cramér-Rao bound, both lower and above [see Fig. 2(b)]. Since this range $[\theta^*, \pi - \theta^*]$ does not depend on the choice of specific observables, we can discuss the tightness of the selection bound quantitatively only by the angles. Because θ^* is given as the arccosine of the ratio between $v_{\text{info}} - v_{\text{info}}^W$ and v_{info}^λ and v_{info} is given as the sum of v_{info}^λ , v_{info}^W and a correlation term between them (cf. *cosine theorem*), θ^* becomes smaller when the contribution of selection v_{info}^λ gets larger, since the ratio gets closer to one. That is, if the contribution of selection is larger than mutation ($v_{\text{info}}^\lambda \gg v_{\text{info}}^W$), then the range becomes wider, so that the selection bound can give a better bound on v_R for a wider variety of observables R . Such a tendency is indeed observed in the numerical calculations below.

B. Complementary result: Mutation bound

The discussion so far has focused on how the evolutionary rate is accelerated by selection on growth. On the other hand, we can discuss acceleration by mutation by inverting the roles of W and λ in the selection bound. Concretely, we can derive the bound

$$v_R^W - v_{\text{info}}^\lambda \leq v_R \leq v_R^W + v_{\text{info}}^\lambda. \quad (17)$$

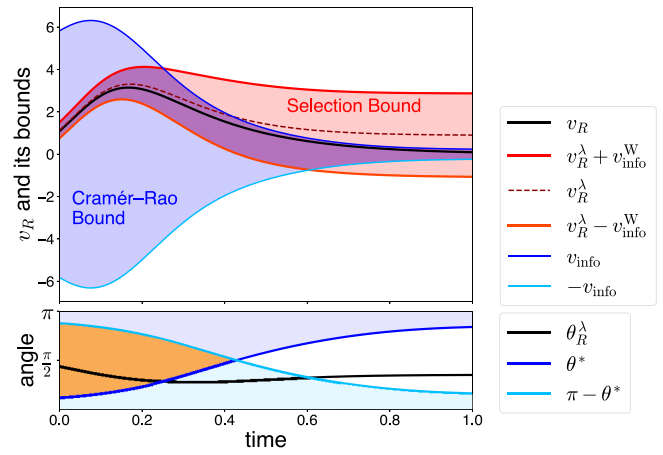


FIG. 3. Numerical calculation for the conventional speed limit (4) by the Cramér-Rao bound and the new speed limit (12) by the selection bound. The horizontal axis is time, and v_R , $v_R^\lambda + v_{\text{info}}^W$, $v_R^\lambda - v_{\text{info}}^W$, v_{info} , and $-v_{\text{info}}$ are plotted in the upper row. The lower row shows the angles, θ_R^λ , θ^* , and $\pi - \theta^*$.

We call this bound *the mutation bound* because it extracts the effect of mutation v_R^W . The same analysis can be performed for the mutation bound as for the selection bound. With both the selection bound and the mutation bound, we can better capture the characteristics of evolutionary processes, especially in the competing situation of natural selection and mutation (see Appendix B for details).

C. Example

We illustrate our results by numerical calculations (Fig. 3). To consider a situation where the contribution of selection is dominant, we have the parameters in (2), $\{\lambda_i\}$ and $\{W_{ij}\}_{i \neq j}$, uniformly sampled from $[-\lambda_{\text{max}}, \lambda_{\text{max}}]$ and $[0, W_{\text{max}}]$, and set $\lambda_{\text{max}}/W_{\text{max}} = 100$. Given that the present results hold for arbitrary time-independent observables, we also uniformly sample $\{R_i\}$ within the range $[-10, 10]$ rather than taking a specific observable. In Fig. 3, at an early stage of the evolutionary dynamics, or far from the steady state, the selection bound better restricts v_R . From the ecological perspective, this behavior seems reasonable: Selection dominantly contributes to the evolutionary processes far from steady states because beneficial mutation gets less likely as evolution progresses. As proven above, the selection bound is tighter than the Cramér-Rao bound when θ_R^λ is in the range $[\theta^*, \pi - \theta^*]$ (in orange in Fig. 3). This range is wider when the selection is dominant. A more precise evaluation of the speed limits is discussed in Appendix C.

D. Experimental accessibility

Our speed limit is quantitatively testable by actual experiments using single-cell lineage tree data. Recent advances in experimental techniques enable us to measure when and into what each cell mutates or divides. For example, by analyzing time-lapse images of growing bacteria [37], we can measure transitions in phenotypic traits (e.g., cell sizes, shapes, and intracellular concentration of a particular protein) and

proliferation dynamics at the same time. The number of individuals with i th trait at time t that have experienced K divisions since time t' , denoted as $N_i(K, t; t')$, can be obtained in such an experiment. This quantity $N_i(K, t; t')$ enables us to compute the instantaneous values of all the quantities in our speed limit, $p_i(t)$, $\hat{\sigma}_i^\lambda$, $\hat{\sigma}_i^W$, $\hat{\sigma}_i$, v_R^λ , v_R^W , v_{info}^λ , and v_{info}^W (see Appendix D). Therefore, we can experimentally check the tightness of our speed limit for arbitrary observable R , which quantifies the contribution of observable R to the evolutionary rate in the selection process.

IV. CONCLUSION

We derived a novel speed limit, the selection bound, that considers the contributions of the selection and mutation separately when the competition between selection and mutation exists. The core of this result is the decomposition of the stochastic entropy change rate into the selection and mutation part. It allows us to understand the limitations of the speeds of observables more precisely than the conventional speed limit from the Cramér-Rao bound. Although the limits from the selection bound depend on the observables we consider, the ‘‘tendency’’ for the selection bound to give a better bound than the Cramér-Rao bound only depends on the selection strength. The selection bound should be effective in selection-dominant situations such as environmental shift conditions.

The decomposition of the stochastic entropy change rate in this paper may be applicable to other nonlinear dynamics. For example, the generalized Lindblad equation for postselection in quantum dynamics [85–87] has a similar nonlinear term originated by the normalization of a probability distribution. Our decomposition into a nonlinear contribution (i.e., selection) and a linear contribution (i.e., mutation) may be generalized for such an equation to derive a specialized speed limit that characterizes the property of postselection.

ACKNOWLEDGMENTS

M.H., J.F.Y., and S.I. thank Shion Orii for valuable discussions. R.N. and S.I. thank Chikara Furusawa and Yusuke Himekoka for helpful comments. S.I. and J.F.Y. also thank Kouki Yamada for valuable discussions. S.I. is supported by JSPS KAKENHI Grants No. 19H05796, No. 21H01560, and No. 22H01141; JST Presto Grant No. JPMJPR18M2; and UTEC-UTokyo FSI Research Grant Program. K.Y. and J.F.Y. are supported by Grant-in-Aid for JSPS Fellows (Grants No. 22J21619 and No. 21J22920, respectively).

M.H. and R.N. contributed equally to this work.

APPENDIX A: EVALUATION OF THE SPEED LIMITS

Here we explain the derivation of Eq. (16). Taking the difference between v_{info} and $v_R^\lambda + v_{\text{info}}^W$, we get $v_{\text{info}} - (v_R^\lambda + v_{\text{info}}^W) = v_{\text{info}} - v_{\text{info}}^W - \cos \theta_R^\lambda v_{\text{info}}^\lambda$. Thus, the following equations hold:

$$\begin{aligned} \cos \theta_R^\lambda &\leq \frac{v_{\text{info}} - v_{\text{info}}^W}{v_{\text{info}}^\lambda} \Rightarrow (v_R \leq) v_R^\lambda + v_{\text{info}}^W \leq v_{\text{info}}, \\ \cos \theta_R^\lambda &\geq \frac{v_{\text{info}} - v_{\text{info}}^W}{v_{\text{info}}^\lambda} \Rightarrow (v_R \leq) v_{\text{info}} \leq v_R^\lambda + v_{\text{info}}^W. \end{aligned} \quad (\text{A1})$$

The same calculations can be applied to the lower limits: $-v_{\text{info}}$ and $v_R^\lambda - v_{\text{info}}^W$. The difference between the two is, $(v_R^\lambda - v_{\text{info}}^W) - (-v_{\text{info}}) = v_{\text{info}} + \cos \theta_R^\lambda v_{\text{info}}^\lambda - v_{\text{info}}^W$. Therefore,

$$\begin{aligned} \cos \theta_R^\lambda &\geq -\frac{v_{\text{info}} - v_{\text{info}}^W}{v_{\text{info}}^\lambda} \Rightarrow -v_{\text{info}} \leq v_R^\lambda - v_{\text{info}}^W (\leq v_R), \\ \cos \theta_R^\lambda &\leq -\frac{v_{\text{info}} - v_{\text{info}}^W}{v_{\text{info}}^\lambda} \Rightarrow v_R^\lambda - v_{\text{info}}^W \leq -v_{\text{info}} (\leq v_R). \end{aligned} \quad (\text{A2})$$

Taking the arccos on both sides of these equations and using the relation $\arccos(-x) = \pi - \arccos(x)$, we obtain Eq. (16) in the main text.

APPENDIX B: DETAIL OF THE MUTATION BOUND

In this section, we describe the results of the numerical calculation for the following speed limit, which we call the mutation bound:

$$v_R^W - v_{\text{info}}^\lambda \leq v_R \leq v_R^W + v_{\text{info}}^\lambda. \quad (\text{B1})$$

This speed limit is expected to give a good evaluation in mutation-dominant situations, whereas the selection bound gives a good evaluation in selection-dominant situations. We below proceed with the discussion in parallel with that in

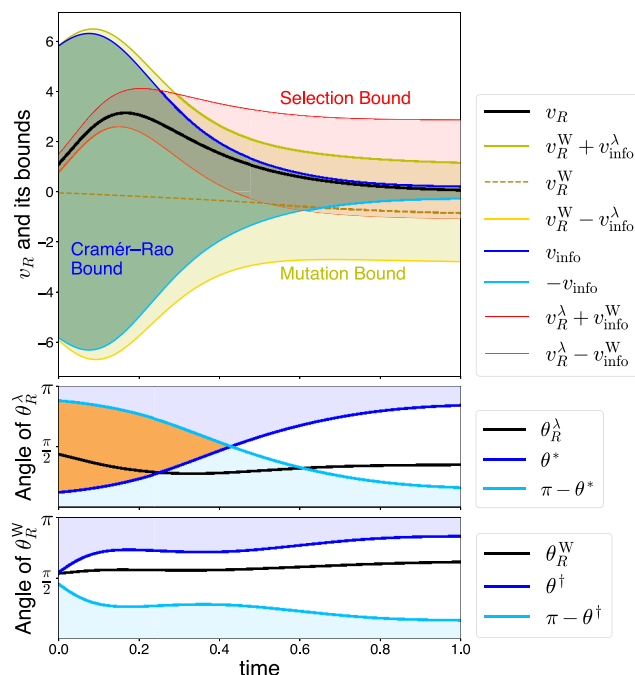


FIG. 4. Numerical calculation of a situation where the selection bound can be tighter for v_R than Cramér-Rao bound and the mutation bound cannot. The horizontal axis is time t and each value is plotted in the upper part of the graph. The lower part shows the angles. The number of species are $n = 10$, the observable R , growth rate λ , and the off-diagonal components of the transition matrix W are taken as uniform random numbers in $[-10, 10]$, $[-10, 10]$, and $[0, 0.1]$, respectively. The initial distribution is also generated as uniform random numbers.

the main text. We define the angle θ_R^W between observable R and the stochastic entropy change rate in the system due to mutation $-\dot{\sigma}^W$ as

$$\theta_R^W = \arccos \left(\frac{\langle \Delta R, -\dot{\sigma}^W \rangle}{\|\Delta R\| \|\dot{\sigma}^W\|} \right) = \arccos \left(\frac{v_R^W}{v_{\text{info}}^W} \right). \quad (\text{B2})$$

Using this angle θ_R^W and another angle θ^\dagger defined as

$$\theta^\dagger := \arccos \left(\frac{v_{\text{info}} - v_{\text{info}}^\lambda}{v_{\text{info}}^W} \right), \quad (\text{B3})$$

the relations among the upper bound $v_{\text{info}}^\lambda + v_R^W$ and the lower bound $-v_{\text{info}}^\lambda + v_R^W$ by the mutation bound and v_{info} are expressed as

$$\begin{aligned} 0 \leq \theta_R^W \leq \theta^\dagger &\Rightarrow v_R \leq v_{\text{info}} \leq v_R^W + v_{\text{info}}^\lambda \\ \theta^\dagger \leq \theta_R^W \leq \pi &\Rightarrow v_R \leq v_R^W + v_{\text{info}}^\lambda \leq v_{\text{info}} \\ 0 \leq \theta_R^W \leq \pi - \theta^\dagger &\Rightarrow -v_{\text{info}} \leq v_R^W - v_{\text{info}}^\lambda \leq v_R \\ \pi - \theta^\dagger \leq \theta_R^W \leq \pi &\Rightarrow v_R^W - v_{\text{info}}^\lambda \leq -v_{\text{info}} \leq v_R. \end{aligned} \quad (\text{B4})$$

In contrast to θ^* , θ^\dagger becomes small when the contribution of mutation to the evolution of the probability distribution is large. It indicates that the range of θ_R^W where the mutation bound is tighter, $[\theta^\dagger, \pi - \theta^\dagger]$, gets wider. To sum up, the

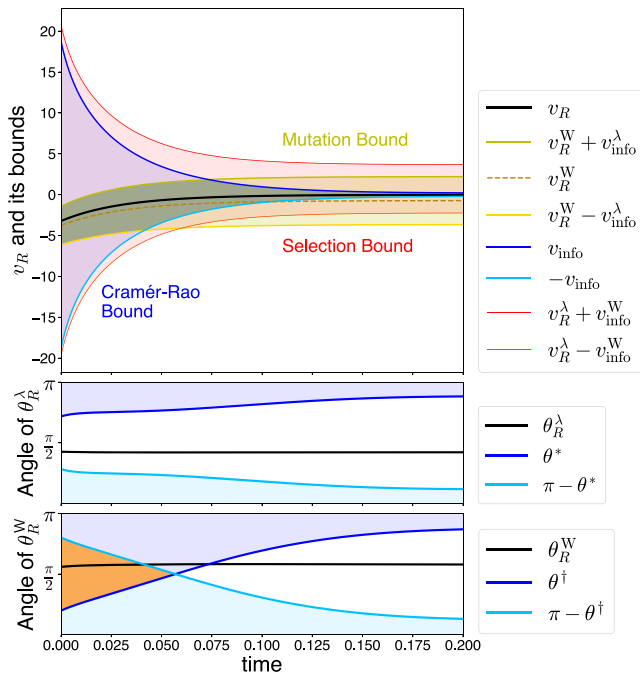


FIG. 5. Numerical calculation of a situation where the mutation bound can be tighter for v_R than Cramér-Rao bound and the selection bound cannot. The horizontal axis is time t and each value is plotted in the upper part of the graph. The lower part shows the angles. Compared to Fig. 4, the parameters are different. The observable R , growth rate λ , transition rate W is generated as uniform random numbers in $[-10, 10]$, $[-5, 5]$, and $[0, 5]$, respectively. Note that the ratio of the growth rate to the mutation rate is 1, not 100 as in Fig. 3 in the main text and Fig. 4.

selection bound gets tighter when the contribution of selection is large, while the mutation bound gets tighter when the contribution of mutation is large.

With the parameters used to demonstrate the selection bound in the main text, the mutation bound gives a loose bound. As shown in Figs. 4 and 5, the mutation bound is loose in situations where the selection bound gives a tight evaluation, and conversely, the selection bound is loose in situations where the mutation bound is tight.

Thus, the selection bound and the mutation bound provide good bounds to evaluate the change speed of the observables in different situations.

APPENDIX C: HOW THE STRENGTH OF SELECTION AND MUTATION AFFECT THE EVALUATION OF THE SPEED LIMITS

In order to evaluate the tightness of the selection bound and the mutation bound quantitatively, we discuss the dependence of the “tendency” to give better limits on the ratio of λ_{max} to W_{max} . This tendency for the selection bound to be tighter than the Cramér-Rao bound can be measured using the value of θ^* . The selection bound gets tighter when the angle θ_R^λ is in the range $[\theta^*, \pi - \theta^*]$. Therefore, if we define $\mathcal{P}^* := \max\{(\pi - 2\theta^*)/\pi, 0\}$, then this \mathcal{P}^* quantifies the tendency of the selection bound to give a better evaluation. The selection bound tends to be tighter when \mathcal{P}^* is close to 1 and looser when \mathcal{P}^* is close to 0. Note that θ^* is not always under $\pi/2$, thus, $\pi - 2\theta^*$ could be negative. In the same way, the tendency of the mutation bound to give a better evaluation can be measured by the value defined as $\mathcal{P}^\dagger := \max\{(\pi - 2\theta^\dagger)/\pi, 0\}$. It is noteworthy that \mathcal{P}^* and \mathcal{P}^\dagger do not depend on the observable R .

We demonstrate the dependence of \mathcal{P}^* and \mathcal{P}^\dagger on the ratio of λ_{max} to W_{max} (see Fig. 6). In the numerical calculation, λ and W is generated by uniform random values in the range $[-\lambda_{\text{max}}, \lambda_{\text{max}}]$, and $[0, W_{\text{max}}]$, respectively. Note here that both \mathcal{P}^* and \mathcal{P}^\dagger depend on time, so we use their values in the initial state of the dynamics. Figure 6 shows that the tendency \mathcal{P}^* of the selection bound to get tighter than the Cramér-Rao bound increases when λ_{max} is larger than W_{max} . This calculation confirms the statement in the main text that the selection bound is effective when natural selection is dominant.

Another finding is that the point where the two curves of \mathcal{P}^* and \mathcal{P}^\dagger intersect is governed by the number of species n . This point represents the ratio $\lambda_{\text{max}}/W_{\text{max}}$ with $v_{\text{info}}^\lambda = v_{\text{info}}^W$. Moreover, the tendency for the selection/mutation bound to give better evaluation swaps at this point. Figure 6 shows that such a ratio is not 1 but close to the number of species n . It implies that the contribution of selection and that of mutation compete when λ_{max} is about n times larger than W_{max} . This fact can be understood by considering a situation where the parameters are $\lambda_i = 1$, $W_{ij} = 1 (i \neq j)$. The contribution to the growth rate of trait i of the selection is 1, whereas the contribution of the mutation is $n - 1$. Therefore, if the traits grow at an identical rate, then the contribution of selection becomes larger in small communities.

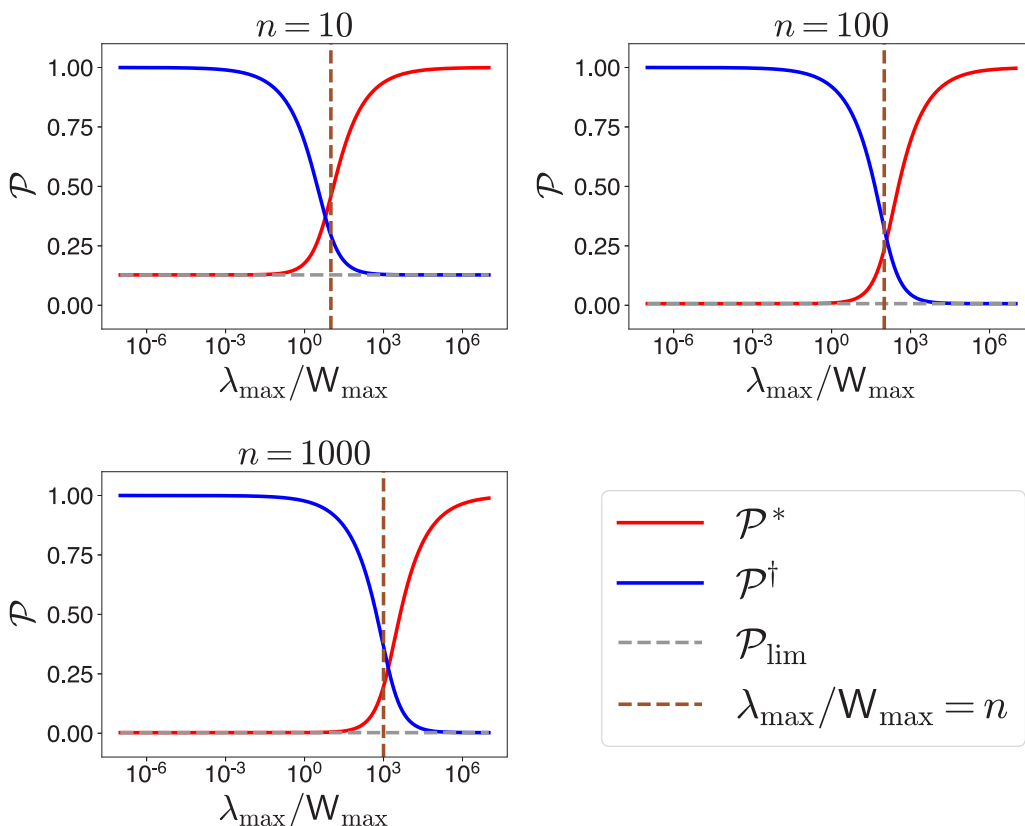


FIG. 6. Numerical calculation for \mathcal{P}^* and \mathcal{P}^\dagger , that quantify the tendency of the selection/mutation bound to get tighter than the Cramér-Rao bound. λ and W are generated by uniform random numbers in $[-\lambda_{\max}, \lambda_{\max}]$ and $[0, W_{\max}]$, respectively. The graphs show how \mathcal{P}^* and \mathcal{P}^\dagger depend on the ratio of λ_{\max} to W_{\max} . \mathcal{P}_{lim} is the limit of \mathcal{P}^* as $\lambda_{\max}/W_{\max} \rightarrow 0$ or that of \mathcal{P}^\dagger as $\lambda_{\max}/W_{\max} \rightarrow \infty$. These two values converge to an identical value, which does not necessarily go to 0. Each graph is the result for a different number of species $n = 10, 100, 1000$.

APPENDIX D: HOW TO VERIFY THE SELECTION BOUND AND THE MUTATION BOUND FROM EXPERIMENTAL DATA

In this section, we describe how one can quantitatively test our speed limit using single-cell genealogical data in the form of population lineage trees which include data of cell divisions and mutations or phenotypic switching (see Fig. 7 as an example). We can compute the number $N_i(K, t; t')$ of individuals with i th trait at time t that have experienced K divisions since time t' from single-cell genealogical data. $N_i(K, t; t')$ enables us to compute the instantaneous values of all the quantities in our speed limit, i.e., $p_i(t)$, σ_i^λ , σ_i^W , and $\dot{\sigma}_i$ as well as v_R^λ , v_R^W , v_{info}^λ , and v_{info}^W for an arbitrary observable R . The details are as follows.

Firstly, from $N_i(K, t; t')$, we define chronological (forward) distribution p^{ch} as

$$p_i^{\text{ch}}(t; t') := \sum_{K=0}^{\infty} \frac{N_i(K, t; t')}{N_{\text{tot}}(t')2^K}. \tag{D1}$$

From these values, we can obtain the instantaneous values of $N_i(t)$ and $p_i(t)$ for each subpopulation: the sum of $N_i(K, t; t')$ with respect to K equals $N_i(t)$,

$$\sum_{K=0}^{\infty} N_i(K, t; t') = N_i(t), \tag{D2}$$

and $p_i^{\text{ch}}(t; t')$ is equal to $p_i(t)$ when $t' = t$,

$$p_i^{\text{ch}}(t; t) = p_i(t), \tag{D3}$$

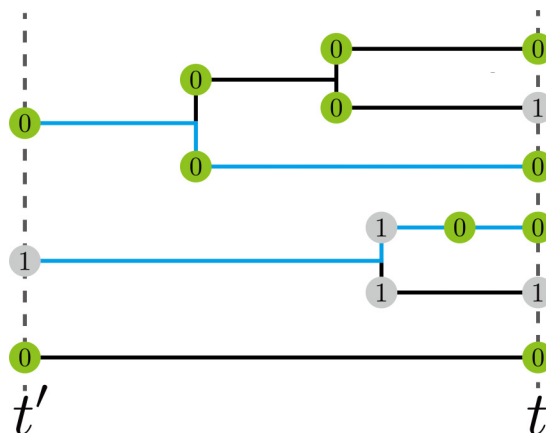


FIG. 7. Example of single-cell lineage trees with two traits, 0 (green) and 1 (gray). The distributions $p(t)$ and $p^{\text{ch}}(t)$ are available only from the cell lineage by counting $N_i(K, t; t')$. The blue lines show the trajectories of individuals that experienced 1 divisions between time t' and t in the subpopulation with the trait 0 at time t . Thus $N_0(1, t; t')$ is 2 in this cell lineage.

because only $K = 0$ is allowed as the number of division between t and t' . Note that the chronological distribution defined above has been studied not only as a theoretical object [40,88] but also utilized to analyze experimental data as in Refs. [37,45]. t' is usually set to the initial time and not explicitly written in these previous studies.

Up to here, we can compute speeds v_R , v_{info} , and $\dot{\sigma}_i$ for any observable R by using $p_i(t)$. On the other hand, since the remaining quantities, v_R^λ , v_R^W , v_{info}^λ , v_{info}^W , $\dot{\sigma}_i^\lambda$, and $\dot{\sigma}_i^W$, depend on the other parameters, λ and W , we need more calculations. Surprisingly, single-cell genealogical data enable us to compute them without estimating the parameters, as we show below.

As a preparation, let us consider the differential equations that $N_i(K, t; t')$ and p^{ch} satisfy. Let an individual with i th trait divide into 2 individuals at rate $r_i \geq 0$. Then, by division, $N_i(K, t; t')$ increases by $2r_i N_i(K-1, t; t')dt$ in an infinitesimal duration dt , while decreasing by $r_i N_i(K, t; t')dt$. Note that only one division can occur in an infinitesimal duration dt . By taking into account the term due to mutation $\sum_{j=1}^n W_{ij} N_j(K, t; t')$, we get the equation

$$\frac{d}{dt} N_i(K, t; t') = 2r_i N_i(K-1, t; t') - r_i N_i(K, t; t') + \sum_{j=1}^n W_{ij} N_j(K, t; t'), \quad (\text{D4})$$

where we define $N_i(K, t; t') = 0$ for $K < 0$. By taking the sum for K , we obtain

$$\frac{d}{dt} N_i(t) = r_i N_i(t) + \sum_{j=1}^n W_{ij} N_j(t). \quad (\text{D5})$$

If we write r_i as λ_i , then it is identical to our model in the main text. Note that r_i is all non-negative, while λ_i can be negative values in general, which reflects the experimental setup that does not account for individual mortality. On the other hand,

combining Eq. (D4) with Eq. (D1), we find

$$\begin{aligned} \frac{d}{dt} p_i^{\text{ch}}(t; t') &= \sum_{K=0}^{\infty} \frac{1}{N_{\text{tot}}(t') 2^K} \left[2r_i N_i(K-1, t; t') \right. \\ &\quad \left. - r_i N_i(K, t; t') + \sum_{j=1}^n W_{ij} N_j(K, t; t') \right] \\ &= r_i \sum_{K=0}^{\infty} \frac{N_i(K-1, t; t')}{N_{\text{tot}}(t') 2^{K-1}} - r_i \sum_{K=0}^{\infty} \frac{N_i(K, t; t')}{N_{\text{tot}}(t') 2^K} \\ &\quad + \sum_{j=1}^n W_{ij} \sum_{K=0}^{\infty} \frac{N_j(K, t; t')}{N_{\text{tot}}(t') 2^K} \\ &= \sum_{j=1}^n W_{ij} p_j^{\text{ch}}(t; t'). \end{aligned} \quad (\text{D6})$$

Now we can present the way to compute $\dot{\sigma}_i^W$ and $\dot{\sigma}_i^\lambda$, using only the distributions $p_i(t)$ and $p_i^{\text{ch}}(t; t')$, which are available from single-cell lineage tree data. Discretizing Eq. (D6) and dividing the obtained equation by $p_i(t)$, we find the relation

$$\frac{p_i^{\text{ch}}(t+dt; t') - p_i^{\text{ch}}(t; t')}{p_i(t) dt} = \sum_{j=1}^n W_{ij} \frac{p_j^{\text{ch}}(t; t')}{p_i(t)}. \quad (\text{D7})$$

Then, substituting t for t' and using Eq. (D3), we see that we can calculate $\dot{\sigma}_i^W$ as

$$\frac{p_i^{\text{ch}}(t+dt; t) - p_i(t)}{p_i(t) dt} = \sum_{j=1}^n W_{ij} \frac{p_j(t)}{p_i(t)} = -\dot{\sigma}_i^W. \quad (\text{D8})$$

On the other hand, if we consider the discretization of Eq. (D5), as we did for Eq. (D6), then we obtain $\dot{\sigma}_i$ as

$$\frac{p_i(t+dt) - p_i(t)}{p_i(t) dt} = \Delta \lambda_i + \sum_{j=1}^n W_{ij} \frac{p_j(t)}{p_i(t)} = -\dot{\sigma}_i. \quad (\text{D9})$$

Then $\dot{\sigma}_i^\lambda$ is given by $\dot{\sigma}_i^\lambda = \dot{\sigma}_i - \dot{\sigma}_i^W$. As a result, it is finally shown that we can compute all the relevant quantities we discuss in the main text from single-cell genealogical data.

[1] M. Kimura, *The Neutral Theory of Molecular Evolution* (Cambridge University Press, Cambridge, UK, 1983).
 [2] T. Ohta, The nearly neutral theory of molecular evolution, *Annu. Rev. Ecol. Syst.* **23**, 263 (1992).
 [3] S. A. Frank, Foundations of social evolution, in *Foundations of Social Evolution* (Princeton University Press, Princeton, NJ, 2019).
 [4] J. Arjan G., M. de Visser, C. W. Zeyl, P. J. Gerrish, J. L. Blanchard, and R. E. Lenski, Diminishing returns from mutation supply rate in asexual populations, *Science* **283**, 404 (1999).
 [5] Y. Wakamoto, J. Ramsden, and K. Yasuda, Single-cell growth and division dynamics showing epigenetic correlations, *Analyst* **130**, 311 (2005).

[6] J. E. Barrick, D. S. Yu, S. H. Yoon, H. Jeong, T. K. Oh, D. Schneider, R. E. Lenski, and J. F. Kim, Genome evolution and adaptation in a long-term experiment with *Escherichia coli*, *Nature* **461**, 1243 (2009).
 [7] J. A. G. M. de Visser and J. Krug, Empirical fitness landscapes and the predictability of evolution, *Nat. Rev. Genet.* **15**, 480 (2014).
 [8] M. Hashimoto, T. Nozoe, H. Nakaoka, R. Okura, S. Akiyoshi, K. Kaneko, E. Kussell, and Y. Wakamoto, Noise-driven growth rate gain in clonal cellular populations, *Proc. Natl. Acad. Sci. USA* **113**, 3251 (2016).
 [9] M. Baym, T. D. Lieberman, E. D. Kelsic, R. Chait, R. Gross, I. Yelin, and R. Kishony, Spatiotemporal microbial evolution on antibiotic landscapes, *Science* **353**, 1147 (2016).

- [10] D. De Martino, F. Capuani, and A. De Martino, Growth against entropy in bacterial metabolism: the phenotypic trade-off behind empirical growth rate distributions in *E. Coli*, *Phys. Biol.* **13**, 036005 (2016).
- [11] B. H. Good, M. J. McDonald, J. E. Barrick, R. E. Lenski, and M. M. Desai, The dynamics of molecular evolution over 60,000 generations, *Nature* **551**, 45 (2017).
- [12] M. Lukačičinová and T. Bollenbach, Toward a quantitative understanding of antibiotic resistance evolution, *Curr. Opin. Biotechnol.* **46**, 90 (2017).
- [13] C. Furusawa, T. Horinouchi, and T. Maeda, Toward prediction and control of antibiotic-resistance evolution, *Curr. Opin. Biotechnol.* **54**, 45 (2018).
- [14] B. Van den Bergh, T. Swings, M. Fauvart, and J. Michiels, Experimental design, population dynamics, and diversity in microbial experimental evolution, *Microbiol. Mol. Biol. Rev.* **82**, e00008 (2018).
- [15] C. Darwin, *On the Origin of Species, 1859* (Routledge, London, 2004).
- [16] R. A. Fisher, *The Genetical Theory of Natural Selection* (Oxford University Press, Oxford, 1958).
- [17] W. J. Ewens, An interpretation and proof of the fundamental theorem of natural selection, *Theor. Popul. Biol.* **36**, 167 (1989).
- [18] S. A. Frank, The price equation, fisher's fundamental theorem, kin selection, and causal analysis, *Evolution* **51**, 1712 (1997).
- [19] J. C. Baez, The fundamental theorem of natural selection, *Entropy* **23**, 1436 (2021).
- [20] S. A. Frank and M. Slatkin, Fisher's fundamental theorem of natural selection, *Trends Ecol. Evol.* **7**, 92 (1992).
- [21] G. R. Price, Extension of covariance selection mathematics, *Ann. Hum. Genet.* **35**, 485 (1972).
- [22] A. Grafen, Developments of the price equation and natural selection under uncertainty, *Proc. R. Soc. Lond. B* **267**, 1223 (2000).
- [23] S. A. Frank, Natural selection. IV. The price equation, *J. Evol. Biol.* **25**, 1002 (2012).
- [24] W. M. Baum, Selection by consequences, behavioral evolution, and the price equation, *J. Exp. Anal. Behav.* **107**, 321 (2017).
- [25] S. A. Frank, The price equation program: Simple invariances unify population dynamics, thermodynamics, probability, information and inference, *Entropy* **20**, 978 (2018).
- [26] S. A. Frank and F. J. Bruggeman, The fundamental equations of change in statistical ensembles and biological populations, *Entropy* **22**, 1395 (2020).
- [27] T. R. Malthus, *An Essay on the Principle of Population* (J. Johnson, London, 1798).
- [28] S. Leibler and E. Kussell, Individual histories and selection in heterogeneous populations, *Proc. Natl. Acad. Sci. USA* **107**, 13183 (2010).
- [29] J. F. Crow and M. Kimura, *An Introduction to Population Genetics Theory, 1970* (Scientific Publishers, New Dehli, 2017).
- [30] W. F. Basener and J. C. Sanford, The fundamental theorem of natural selection with mutations, *J. Math. Biol.* **76**, 1589 (2018).
- [31] K. Sekimoto, *Stochastic Energetics* (Springer, Berlin, 2010), Vol. 799.
- [32] U. Seifert, Stochastic thermodynamics, fluctuation theorems and molecular machines, *Rep. Prog. Phys.* **75**, 126001 (2012).
- [33] S. H. Strogatz, *Nonlinear Dynamics and Chaos: With Applications to Physics, Biology, Chemistry, and Engineering* (CRC Press, Boca Raton, FL, 2018).
- [34] Y. Wakamoto, A. Y. Grosberg, and E. Kussell, Optimal lineage principle for age-structured populations, *Evolution* **66**, 115 (2012).
- [35] G. Lambert and E. Kussell, Quantifying Selective Pressures Driving Bacterial Evolution Using Lineage Analysis, *Phys. Rev. X* **5**, 011016 (2015).
- [36] M. Hoffmann and A. Olivier, Nonparametric estimation of the division rate of an age dependent branching process, *Stoch. Process. Appl.* **126**, 1433 (2016).
- [37] T. Nozoe, E. Kussell, and Y. Wakamoto, Inferring fitness landscapes and selection on phenotypic states from single-cell genealogical data, *PLoS Genet.* **13**, e1006653 (2017).
- [38] B. Andrae, J. Cremer, T. Reichenbach, and E. Frey, Entropy Production of Cyclic Population Dynamics, *Phys. Rev. Lett.* **104**, 218102 (2010).
- [39] H. Qian, Fitness and entropy production in a cell population dynamics with epigenetic phenotype switching, *Quant. Biol.* **2**, 47 (2014).
- [40] T. J. Kobayashi and Y. Sughiyama, Fluctuation Relations of Fitness and Information in Population Dynamics, *Phys. Rev. Lett.* **115**, 238102 (2015).
- [41] Y. Sughiyama, T. J. Kobayashi, K. Tsumura, and K. Aihara, Pathwise thermodynamic structure in population dynamics, *Phys. Rev. E* **91**, 032120 (2015).
- [42] Y. Sughiyama and T. J. Kobayashi, Steady-state thermodynamics for population growth in fluctuating environments, *Phys. Rev. E* **95**, 012131 (2017).
- [43] T. J. Kobayashi and Y. Sughiyama, Stochastic and information-thermodynamic structures of population dynamics in a fluctuating environment, *Phys. Rev. E* **96**, 012402 (2017).
- [44] R. García-García, A. Genthon, and D. Lacoste, Linking lineage and population observables in biological branching processes, *Phys. Rev. E* **99**, 042413 (2019).
- [45] A. Genthon and D. Lacoste, Fluctuation relations and fitness landscapes of growing cell populations, *Sci. Rep.* **10**, 11889 (2020).
- [46] A. Genthon and D. Lacoste, Universal constraints on selection strength in lineage trees, *Phys. Rev. Res.* **3**, 023187 (2021).
- [47] K. Yoshimura and S. Ito, Thermodynamic Uncertainty Relation and Thermodynamic Speed Limit in Deterministic Chemical Reaction Networks, *Phys. Rev. Lett.* **127**, 160601 (2021).
- [48] A. Kolchinsky, A thermodynamic threshold for Darwinian evolution, [arXiv:2112.02809](https://arxiv.org/abs/2112.02809).
- [49] M. Esposito and C. Van den Broeck, Three faces of the second law. I. Master equation formulation, *Phys. Rev. E* **82**, 011143 (2010).
- [50] C. Van den Broeck and M. Esposito, Three faces of the second law. II. Fokker-Planck formulation, *Phys. Rev. E* **82**, 011144 (2010).
- [51] A. C. Barato and U. Seifert, Thermodynamic Uncertainty Relation for Biomolecular Processes, *Phys. Rev. Lett.* **114**, 158101 (2015).
- [52] Z. Zhang, S. Guan, and H. Shi, Information geometry in the population dynamics of bacteria, *J. Stat. Mech.: Theory Exp.* (2020) 073501.
- [53] G. E. Crooks, Measuring Thermodynamic Length, *Phys. Rev. Lett.* **99**, 100602 (2007).
- [54] S. Ito, Stochastic Thermodynamic Interpretation of Information Geometry, *Phys. Rev. Lett.* **121**, 030605 (2018).

- [55] L. Mandelstam and I. G. Tamm, The uncertainty relation between energy and time in non-relativistic quantum mechanics, in *Selected Papers* (Springer, Berlin, 1991), pp. 115–123.
- [56] J. Anandan and Y. Aharonov, Geometry of Quantum Evolution, *Phys. Rev. Lett.* **65**, 1697 (1990).
- [57] N. Margolus and L. B. Levitin, The maximum speed of dynamical evolution, *Physica D* **120**, 188 (1998).
- [58] M. M. Taddei, B. M. Escher, L. Davidovich, and R. L. de Matos Filho, Quantum Speed Limit for Physical Processes, *Phys. Rev. Lett.* **110**, 050402 (2013).
- [59] D. P. Pires, M. Cianciaruso, L. C. Céleri, G. Adesso, and D. O. Soares-Pinto, Generalized Geometric Quantum Speed Limits, *Phys. Rev. X* **6**, 021031 (2016).
- [60] B. Shanahan, A. Chenu, N. Margolus, and A. del Campo, Quantum Speed Limits Across the Quantum-to-Classical Transition, *Phys. Rev. Lett.* **120**, 070401 (2018).
- [61] M. Okuyama and M. Ohzeki, Quantum Speed Limit is not Quantum, *Phys. Rev. Lett.* **120**, 070402 (2018).
- [62] S.-i. Amari, *Information Geometry and Its Applications* (Springer, Berlin, 2016), Vol. 194.
- [63] S. Ito and A. Dechant, Stochastic Time Evolution, Information Geometry, and the Cramér–Rao Bound, *Phys. Rev. X* **10**, 021056 (2020).
- [64] S. B. Nicholson, L. P. Garcia-Pintos, A. del Campo, and J. R. Green, Time–information uncertainty relations in thermodynamics, *Nat. Phys.* **16**, 1211 (2020).
- [65] K. Yoshimura and S. Ito, Information geometric inequalities of chemical thermodynamics, *Phys. Rev. Res.* **3**, 013175 (2021).
- [66] S. Ito, Information geometry, trade-off relations, and generalized glansdorff–prigogine criterion for stability, *J. Phys. A: Math. Theor.* **55**, 054001 (2022).
- [67] K. Ashida, K. Aoki, and S. Ito, Experimental evaluation of thermodynamic speed limit in living cells via information geometry, (2021), doi: [10.1101/2020.11.29.403097](https://doi.org/10.1101/2020.11.29.403097).
- [68] C. R. Rao, Information and the accuracy attainable in the estimation of statistical parameters, in *Breakthroughs in Statistics* (Springer, Berlin, 1992), pp. 235–247.
- [69] K. Sato, Y. Ito, T. Yomo, and K. Kaneko, On the relation between fluctuation and response in biological systems, *Proc. Natl. Acad. Sci. USA* **100**, 14086 (2003).
- [70] P. Michel, S. Mischler, and B. Perthame, General relative entropy inequality: An illustration on growth models, *J. Math. Pures Appl.* **84**, 1235 (2005).
- [71] D. M. Wolf, V. V. Vazirani, and A. P. Arkin, Diversity in times of adversity: Probabilistic strategies in microbial survival games, *J. Theor. Biol.* **234**, 227 (2005).
- [72] E. Kussell and S. Leibler, Phenotypic diversity, population growth, and information in fluctuating environments, *Science* **309**, 2075 (2005).
- [73] O. Rivoire and S. Leibler, The value of information for populations in varying environments, *J. Stat. Phys.* **142**, 1124 (2011).
- [74] S. A. Frank, Natural selection. V. How to read the fundamental equations of evolutionary change in terms of information theory, *J. Evol. Biol.* **25**, 2377 (2012).
- [75] S. A. Frank, Natural selection. VI. Partitioning the information in fitness and characters by path analysis, *J. Evol. Biol.* **26**, 457 (2013).
- [76] K. Kaneko, C. Furusawa, and T. Yomo, Universal Relationship in Gene-Expression Changes for Cells in Steady-Growth State, *Phys. Rev. X* **5**, 011014 (2015).
- [77] B. Xue and S. Leibler, Benefits of phenotypic plasticity for population growth in varying environments, *Proc. Natl. Acad. Sci. USA* **115**, 12745 (2018).
- [78] S. Nakashima and T. J. Kobayashi, Acceleration of evolutionary processes by learning and extended fisher’s fundamental theorem, *Phys. Rev. Res.* **4**, 013069 (2022).
- [79] K. Adachi, R. Iritani, and R. Hamazaki, Universal constraint on nonlinear population dynamics, *Commun. Phys.* **5**, 129 (2022).
- [80] L. P. Garcia-Pintos, Diversity and fitness uncertainty allow for faster evolutionary rates, [arXiv:2202.07533](https://arxiv.org/abs/2202.07533).
- [81] We remark that the Cramér–Rao bound holds even for time-dependent observables by changing the definition of v_R as $v_R = (d_t \langle R \rangle - \langle d_t R \rangle) / \sqrt{\text{Var}[R]}$.
- [82] T. M. Cover, *Elements of Information Theory* (John Wiley & Sons, New York, 1999).
- [83] S. A. Frank, Natural selection maximizes fisher information, *J. Evol. Biol.* **22**, 231 (2009).
- [84] We remark that a similar concept of the angle can be seen in the Price equation [23].
- [85] H. M. Wiseman, Quantum trajectories and feedback, Ph.D. thesis, University of Queensland, 1994.
- [86] J. D. Cresser, S. M. Barnett, J. Jeffers, and D. T. Pegg, Measurement master equation, *Opt. Commun.* **264**, 352 (2006).
- [87] Y.-N. Zhou, Generalized Lindblad master equation for measurement-induced phase transition, *SciPost Phys. Core* **6**, 023 (2023).
- [88] E. Baake and H.-O. Georgii, Mutation, selection, and ancestry in branching models: A variational approach, *J. Math. Biol.* **54**, 257 (2007).